

**Showcasing research from Professor Bishwajit Ganguly's laboratory, CSIR-Central Salt and Marine Chemical Research Institute, Bhavnagar, India.**

Crystal habit modification of sodium chloride using habit modifiers: a dive into more than 50 years of research & development on crystal habit modification of rock-salt crystals

The control of crystal morphology is of paramount importance in industries and in pharmaceuticals, as the morphological features of crystals play pivotal role in flow abilities, stability and dissolution properties etc. The morphological changes in crystals occurred by the rate of cooling, supersaturation, solvent effect, temperature, pressure or adding impurity as a habit modifier. This article highlights the development in the habit of sodium chloride crystals using impurities as a controlling factor and the advancement that has taken place in this domain of research for over the years.

Image reproduced by permission of Bishwajit Ganguly from *CrystEngComm*, 2025, **27**, 2439.

**As featured in:**





See Sumit Kumar Pramanik and Bishwajit Ganguly, *CrystEngComm*, 2025, **27**, 2439.



Cite this: *CrystEngComm*, 2025, 27, 2439

# Crystal habit modification of sodium chloride using habit modifiers: a dive into more than 50 years of research & development on crystal habit modification of rock-salt crystals

Sumit Kumar Pramanik <sup>\*ab</sup> and Bishwajit Ganguly <sup>\*ab</sup>

Crystal habit modification of salt crystals has been a fascinating area of research for decades. The microscopic analysis of drops of brine evaporating in air showed crystal forms of sodium chloride other than the cube when crystal habit modifiers were added to the brine solution. Some of these additives have a marked effect on salt crystals with definite morphology. This review article covers the role of several parameters in the changes in the morphology of salt crystals. The molecular-level understanding of the crystal growth of sodium chloride crystals has been discussed. Selective crystal habit modification using crystal habit modifiers provides a strategy to generate the desired crystal shapes that may circumvent the problems associated with the salt manufacturing industries. In this review, the in-depth understanding of the role of the crystal habit modifiers in the crystallization process or crystal agglomeration has been discussed for improvement in various industrial and bio-medical applications.

Received 14th October 2024,  
Accepted 24th December 2024

DOI: 10.1039/d4ce01055h

rsc.li/crystengcomm

## 1. Introduction

Crystals often exhibit unusual yet beautiful geometric shapes and morphologies. Their iridescent appearance,

coupled with unique physicochemical and structural properties, make them important materials for a variety of industrial and biomedical applications. Until the 19th century, the primary application of crystals was limited to jewellery. Various single crystals of minerals formed in the geologic past over hundreds to millions of years are found in mines and caves worldwide. In addition to natural sources, currently, most crystals are artificially made to

<sup>a</sup> CSIR – Central Salt and Marine Chemicals Research Institute, Gijubhai Badheka Marg, Bhavnagar, Gujarat 364002, India. E-mail: sumitpramanik@csmcri.res.in

<sup>b</sup> Academy of Scientific and Innovative Research (AcSIR), Ghaziabad 201002, India



Sumit Kumar Pramanik

Sumit Kumar Pramanik is a senior scientist at CSIR-CSMCRI, Bhavnagar, India, and assistant professor at AcSIR. He received his BSc in chemistry from Vidyasagar University and a Master's degree in applied chemistry from Bengal Engineering and Science University. He obtained his PhD in Chemistry from CSIR-Indian Institute of Chemical Biology, Kolkata. He performed postdoctoral research at the

Hasselt University, Belgium. Research in the Sumit group focuses on synthesis, self-assembly, colloidal and interfacial properties, and application of nanostructured materials in bioimaging, drug delivery, sensing, and optoelectronics.



Bishwajit Ganguly

Bishwajit Ganguly is a chief scientist at CSIR-CSMCRI, Bhavnagar, India, and professor at AcSIR. He obtained his PhD from Indian Institute of Science, Bengaluru and his research group focuses on solving contemporary research problems using computational methods.

satisfy the needs of science and technology, as well as jewellery.

Crystallization is a process employed in the manufacturing of a broad range of bulk commodity chemicals and is also used in the preparation of specialty chemicals and pharmaceuticals. The crystallization process resulted in attaining purity and crystal size distribution in many chemical and pharmaceutical applications.<sup>1–3</sup> In the context of crystallography, the term morphology (or habit) denotes the visible presence of a crystal characterized by a set of surfaces and their relative areas.<sup>4,5</sup> A crystal is restricted entirely by faces, and the general shape of the crystal is called the crystal habit or the morphology.<sup>6–8</sup>

A polymorph is a solid crystalline phase of a particular compound resulting from at least two different arrangements of the molecules of that compound in the solid state.<sup>9–11</sup> One of the well-known examples of polymorphism is the ability of any element or molecule to crystallize into many unique crystal species (for example, carbon as hexagonal graphite or cubic diamond).<sup>9</sup> Tautomers or geometrical isomers cannot be called polymorphs, although may behave in a confusingly similar manner. Various polymorphs of a given compound possess different structures and properties. Solubility, melting point, density, crystal shape, hardness, vapor pressure, optical and electrical properties, *etc.*, all differ with the polymorphic form.<sup>11</sup> Meanwhile crystal habit refers to the external appearance of a crystal with a different crystal shape or crystal morphology.<sup>12–14</sup> It can be altered by the growth conditions during the recrystallization process. In general terms, a crystal face with a large area will correspond to a slower growth rate perpendicular to the plane of that face, while faces with small areas indicate faster crystal growth in a perpendicular direction.<sup>15,16</sup> Lower concentrations of impurities have been employed for crystal habit modification.<sup>16</sup>

To precisely control particle shapes, industrial crystallization techniques utilized crystal habit modifiers to achieve the desired crystal shape.<sup>17</sup> In this process, the crystals are grown in the presence of naturally occurring soluble additives that can either adsorb or bind to the crystal faces, influencing the crystal growth and morphology.<sup>18,19</sup> This is how crystal habit modifiers can bring about relatively diverse variations in crystal shapes.<sup>15</sup> However, the shape change mechanisms for particles crystallized with crystal habit modifiers are still unidentified, as these crystallization techniques involve several sequences of trial and error processes to attain the desired crystal shapes. This problem stems from the inadequate molecular-level understanding of crystal growth mechanisms.

With the development of hardware and software, quantum chemical and molecular dynamics simulations are now at the forefront in many areas including salt crystallization. Molecular dynamics simulations have shed light on the cluster growth and the role of solvent in the crystallization process and help to understand the mechanisms at the molecular level to achieve the desired goals.<sup>20,21</sup> MD

simulation studies have further been extended to examine the growth of sodium chloride crystals in supersaturated solutions and the findings show that NaCl crystals grow as clusters in the solution, however, not uniformly on the existing seed crystals. This result was found to be in contrast to the growth from a NaCl melt.<sup>22</sup>

Sodium chloride (NaCl), commonly known as table salt, has long been a focus of study in crystallography due to its simple ionic structure and high availability. NaCl crystal modification is crucial for industry because it enables the tailoring of the material's properties to meet specific application needs. By altering crystal size, shape, structure, or incorporating defects, NaCl can be optimized for use in diverse sectors such as food, pharmaceuticals, and chemical processing. For example, modified crystals improve dissolution rates in food production, enhance reactivity in chemical synthesis, and serve as transparent substrates in optical devices. Additionally, studying these modifications helps develop advanced materials and processes, contributing to innovations in energy, environmental sustainability, and manufacturing technologies.

NaCl serves as a model system for studying crystal growth and modification processes. Its cubic structure, well-characterized crystallization behavior, and responsiveness to additives make it an ideally suited material for understanding the environmental conditions and chemical agents that influence crystal morphology.<sup>23</sup> This research is particularly valuable for developing advanced materials and improving processes in fields like materials science, chemistry, and industrial manufacturing. NaCl can give insights into the area of morphology with additives that can be broadly applied to other ionic compounds and crystal systems.

This highlight begins with introducing the general concept of crystal habit modification. Further, it describes the molecular-level understanding of the crystal growth of NaCl in the presence of crystal habit modifiers. The recently developed theoretical models and computational results to assist and predict the morphology of NaCl crystals have been discussed. The efforts of correlating experimental and computational studies have provided new qualitative insights into the role of habit modifiers in shaping the morphology of salt crystals. Finally, we summarize the existing challenges for the selection of habit modifiers to guide and minimize trial-and-error experiments, streamlining the process of achieving the desired crystal morphology.

### 1.1. Proposed concepts for habit modification

The morphology of a crystal is dependent on the various crystallographic faces that grow under the experimental conditions. Faces that grow rapidly often have minimal impact on the overall crystal shape, while the slow-growing faces exert a larger influence on its morphology. The growth rate of a specific face is influenced both by the crystal's internal structure and defects, as well as by external

environmental conditions. The crystal growth rate is directed by two factors: internal factors, including structural and morphological influences, and external factors, including temperature, impurities, supersaturation, and the presence of solvents.<sup>7,24</sup> Early efforts to explain the wealth of individual crystal shapes were based only on internal factors, employing the type and parameters of the crystallographic unit cell.<sup>23,25</sup> The initial attempt to relate the crystal habit to the lattice geometry was based on the Bravais–Friedel–Donnay–Harker (BFDH) law.<sup>26,27</sup> According to the BFDH rule, the interplanar distance  $d_{hkl}$  governs the morphology of a pure crystal.<sup>5</sup> The important faces in the crystal morphology appeared with the highest reticular densities and the largest interplanar distances,  $d_{hkl}$ . Despite its low precision, it is still used as a preliminary approach in determining the crucial faces of a grown crystal or carrying out the first estimation of a crystal shape. First, in 1955, the periodic bond chain (PBC) theory was introduced by Hartman and Perdok, giving the idea about the relations among the structure and morphology of crystals.<sup>28,29</sup> The morphology of a crystal has been derived using the periodic bond chain (PBC) theory to obtain the structural information of the building units and their interactions in the unit cell.<sup>28,29</sup> The morphological theory of PBC has considered the involvement of bond energies in integrating growth units into the crystal lattice. The periodic chains of bonds are built between the first neighbour interaction units – the so-called connected nets, and as the number of strong bonds per unit cell is limited, there exists a maximum length for the period of a PBC and, hence, a limited number of PBCs.<sup>30</sup> The growth layer of minimum thickness is the elementary “slice”, denoted as  $d_{hkl}$ . The faces that start growing slice after slice are termed as flat or F-faces. For a slice to form, the two adjacent parallel periodic bond chains should be bonded together by strong bonds (Fig. 1a).<sup>31</sup> If this bonding does not occur, no slice can form, and layer growth is not possible; such faces are termed stepped or S-faces (Fig. 1b). If no periodic bond chain exists within a layer of thickness  $d_{hkl}$ , the face is classified as

kinked or K-face, which does not require nucleation for growth as it represents a generalized form of Kessel's repeatable step (Fig. 1c). Thus, the PBC model states that for crystal structure-dependent growth, the morphology should ideally be defined by F-faces, though not all F-faces need to be present. A few reported examples of the use of PBC analysis to predict crystal morphology include hexamethylenetetramine, calcium sulfate, anthracene, magnesium hydrogen phosphate, sodium sulphite, potassium sulfate, and succinic acid.<sup>31</sup>

Later, Docherty and Roberts (1988) introduced an alternative method involving the calculation of surface attachment energies.<sup>32</sup> According to this technique, faces with the lowest attachment energies grow the slowest and thus become the most prominent in the crystal's morphology (Bennema and Hartman, 1980).<sup>30</sup> This approach effectively modeled the theoretical shapes of various molecular crystals, including anthracene, biphenyl, and  $\beta$ -succinic acid. Similarly, Clydesdale and Roberts (1991) predicted the structural stability and morphologies of crystalline C18–C28 *n*-alkanes.<sup>12</sup> Anwar and Boateng (1998) demonstrated how crystallization from solution can be simulated using molecular dynamics for a model solute/solvent system with atomic species characterized by the Lennard-Jones potential function.<sup>25</sup> Comprehensive accounts of molecular modeling techniques, including computer simulations and computational chemistry, can be found in studies by Docherty and Meenan (1999) and Myerson (1999).<sup>33</sup> Besides internal factors, the morphology of crystals is also determined by external factors, *i.e.*, growth conditions.<sup>34</sup> The morphology of a crystal depends on the relative growth rates of the different crystallographic faces.<sup>35</sup> The faster the growth in a given direction, the smaller the face develops and less important it is to control the morphology of a crystal.

Besides other external parameters, crystal growth also depends strongly on the impurities present in the crystal lattice, including supersaturation and temperature. In 1933, Prof. Bunn proposed that for strong absorption, the atomic arrangement in the absorbing face of the host crystal must correspond to that in a face in crystals of the habit-modifying substance.<sup>36,37</sup> This implies that the absorbed particles need to lie on the crystal surface in almost the same way as it would be stable if these particles were to crystallize alone.<sup>36,38</sup> If substance X modifies the habit of Y, a reversal is anticipated unless the atomic arrangement of X, which is analogous to that of a plane in Y, exists on a face already prominent in X. In that particular circumstance, it would be impossible to predict if the prominence of the face has been affected by the presence of Y.

To influence the morphology of crystals, tailor-made additives have been designed to fit at particular surface locations and thus affect the growth of specific crystallographic faces.<sup>39</sup> If the crystals are grown in sterile solutions, they grow with regular, monomolecular surface steps.<sup>39</sup> The addition of additives to a growth solution often generates irregular macrosteps, which develop the inclusion

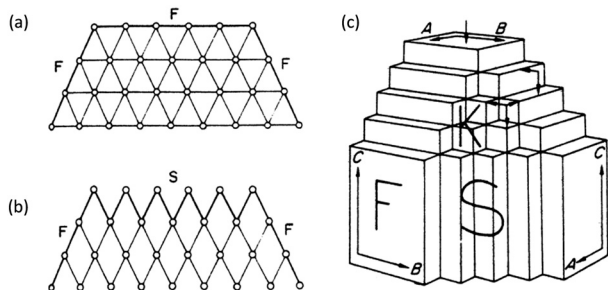


**Fig. 1** (a) and (b) Projection of a three-dimensional crystal along a PBC. Each circle represents a PBC. The F-face results when neighbouring PBCs are linked together by strong bonds, otherwise the S-face develops. (c) Crystal with three PBCs parallel to [100] (A), [010] (B), and [001] (C). The F-faces are (100), (010) and (001). The S-faces are (110), (101) and (011). The K-face is (111). Reproduced with permission from ref. 31. Copyright 2001 Elsevier Ltd.

## Highlight

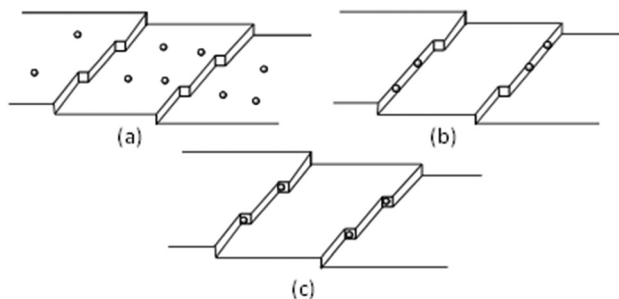


Fig. 2 Sites for impurity adsorption on a growing crystal, based on the Kossel model; (a) flat, (b) step, and (c) kink.

of liquid.<sup>40</sup> Over the decades, many models describing the effect of impurities on the crystal growth process have been based on the concept of adsorption of contaminants (such as inorganic ions, atoms, or molecules) at flat, steps and kink faces of a growing surface. The Kossel model shows the three sites of adsorption of impurities on a growing surface (Fig. 2).

“Cabrera and Vermilyea” hypothesized a mechanism based on the existence of strongly adsorbed impurity particles distributed all over the crystal surface.<sup>41</sup> If the transmitting growth step hits such a particle, it stops at that point and tries to move around it, resulting in a distortion of the step edge and, subsequently, impeding the growth velocity. Bliznakov proposed the model of reduction of growth sites on the face, and the reported experimental results supported this model for a number of water-soluble compounds.<sup>42</sup> Sears,<sup>43</sup> Dunning, and Albon<sup>44</sup> also introduced the model of adsorption of impurity molecules at the flat face (F) and tested the validity of their model against the dependence of rates of motion of the growth layer on impurity concentration. The second phase of investigations on impurity effects started from the work of Davey and Mullin.<sup>45,46</sup> The study was performed with the layer displacement rates as a function of impurity concentration and tested the experimental data with the models of impurity adsorption. NaCl is known to be one of the first crystals for which the effect of impurity was detected and investigated.

### 1.2. Strategies to design impurity/additives

The crystal growth morphology has various applications ranging from drug design for regenerative medicine to explosives and industrial chemistry. The application of habit modification in salt technology is one of the important areas of research. The effects of NaCl crystal shape and size strongly influence washing, filtering, and drying as well as mechanical strength, storage, *etc.* The crystal growth mostly depends on two factors, the internal factor and the external factors like additives, temperature, pH, supersaturation, and solvent effects. To date, several computational and experimental studies have been performed to recognize the properties of additives such as lattice fit, multipoint adsorption, and conformations of the additives, that induce

the habit modification in NaCl crystals. Some of the predicted results have been corroborated with the experimental results. However, the selection of such impurities is largely empirical and there are no rational approaches. Recently, it has been proposed that parameters that can qualitatively indicate the efficiency of tested additives qualify as organic habit modifiers for NaCl crystals.<sup>47</sup>

The adsorption phenomenon of additives on NaCl faces was found as an important parameter to induce the morphological change in salt crystals. NaCl is hydrophilic and therefore highly soluble in water. Hence, the degree of hydrophilicity of impurity/additives will be an important parameter to induce habit modification of NaCl crystals. The miscibility of impurity/additives in the solution was measured with the hydrophilic/hydrophobic parameter, determined from the partition coefficient ( $\log P$ ) value.<sup>47</sup> The scale of  $\log P$  indicates the hydrophilicity of the system with high (–)ve values and the hydrophobicity with (+)ve values. The earlier reports indicate that the impurity/additives with glycine, urea, formamide, creatinine, cysteine, citric acid, and barbituric acid with (–)ve  $\log P$  values can act as NaCl habit modifiers, whereas the impurity/additives with low negative or positive  $\log P$  values work as non-habit modifiers like thiourea, *N,N*-dimethyl-formamide, benzamide, phenol, pyridine, acetic acid and aniline.<sup>47,48</sup> The experimental and computational results shed light on the importance of a fundamental principle to address the role of electronic and structural features of the additive in tuning the morphology of NaCl crystals.

### 1.3. Role of additives in the morphology of NaCl crystals

Literature reports reveal the cube–octahedron shape transition for various experimental conditions. In 1783, Rome de l'Isle reported the influence of urea on the growth morphology of NaCl in the book *Crystallography* and ignited interest in the area of crystallography. The experimental results conclude that common salt forms octahedral crystals instead of cubes from brine containing about 30 wt% (with respect to solute) of urea. There are reports available suggesting that adding inorganic salts, such as  $\text{CdCl}_2$ ,  $\text{ZnCl}_2$ , and  $\text{MnCl}_2$ , forms octahedral crystals for common salt.<sup>49</sup> Since NaCl is crucial to life on Earth, therefore, it has attracted the attention of researchers for decades. It is an essential ingredient in the diets of people and animals, though it plays a vital role in various industrial processes as well. There are many reports on the growth and morphology of NaCl crystals. However, the control of morphology remained mainly a matter of ‘mix and try’. In the 1950s–60s, some studies were performed in which the morphology of NaCl crystals grown from aqueous solutions was determined as a function of impurity concentration. For NaCl crystals, the stable crystallographic face changed from {100} to {111} and {110} planes with impurity leading to octahedron and rhombic dodecahedron forms, respectively.<sup>50</sup> Although these

facts have been known about the habit modification of NaCl, there was hardly any comprehensive and unifying theory that could explain all these facts. From time to time, attempts have been made to explain specific examples of the general effect. Royer (1934) attempted to explain the action of inorganic ions ( $\text{CdCl}_2$ ,  $\text{MnCl}_2$ ,  $\text{ZnCl}_2$ ) in producing octahedral  $\{111\}$  faces on NaCl by pointing out that these divalent chlorides have  $\{111\}$  faces with dimensions very close to the  $\{111\}$  face of NaCl.<sup>51</sup> It is speculated that this particular structural feature encouraged the development of the  $\{111\}$  faces in the salt crystal and thus brought about an octahedral form. Bunn (1933) explained the habit-modifying action of urea on salt by postulating that an unstable mixed crystal of the materials formed on the affected face.<sup>36</sup> Conditions for the intense absorption necessary for the formation of the mixed crystal are the similarity of lattice structure and interatomic distances on specific planes only; the rest of the network can be entirely dissimilar. Palm and MacGillavry (1963) have produced evidence to suggest that the adsorption of NaCl, urea, and  $\text{H}_2\text{O}$  on the crystal surface is responsible for the morphological changes of NaCl.<sup>52</sup> Hille and Jentsch (1963) have concluded that urea produced its effect by encouraging the adsorption of water molecules onto the  $\{111\}$  face of NaCl.<sup>53</sup> Speidel (1961), in attempting to explain the different effects of glycine, acetic acid, alanine, and formamide on salt, introduced the concept that charge distribution in the molecule plays a part as well as the “fit” of the molecule onto a lattice in determining its adsorption onto the surface of a crystal.<sup>5</sup>

Cabrera (1958) considered that impurity is strongly adsorbed onto the relevant face of the crystal and forms a “jacket” that encloses the growth of steps.<sup>41</sup> The growth rate will fall if the mean distance between impurity particles is comparable with the size of the two-dimensional nucleus for the overall supersaturation. This mechanism is only possible if the lifetime of the adsorption is longer than the time needed for a growth step to move the distance between impurity particles. This implies that, for effective adsorption of impurity onto the crystal surfaces, adsorption energy should be high. Many proposals and theories have been put forward, but there is a lack of fundamental understanding of the microscopic mechanisms behind this effect.

NaCl cubic single crystals are crystallized in a common habit with the competing growth rate of  $\{100\}$  and  $\{111\}$  faces. In 1990, Prof. Lian *et al.* revealed nicely how the morphology of NaCl can be altered by changing the relative growth rate of  $\{100\}$  and  $\{111\}$  faces.<sup>54</sup> NaCl crystals with octahedron or dodecahedron shape morphology are obtained by hindering the relative growth rate of the  $\{111\}$  or  $\{110\}$  crystallographic faces, respectively. The electrostatically polar  $\{111\}$  surface of NaCl, where the bulk structure comprises alternating sheets of cations and anions along the  $\langle 111 \rangle$  direction, has been computed to be unstable theoretically.<sup>55</sup> Recently, Enckevort *et al.* have performed studies on the impact of impurities in the growth solution on the structure and growth of the NaCl crystal surface, aiming at a better

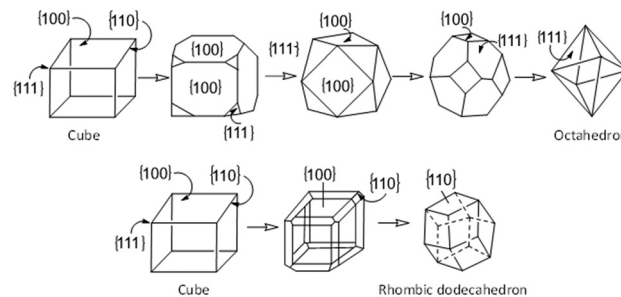
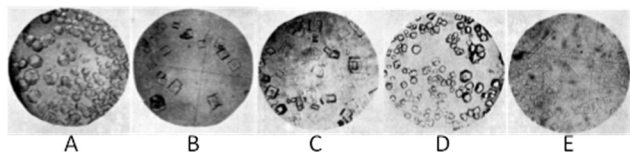


Fig. 3 The progressive change of alkali halide crystals from cube to octahedron and rhombic dodecahedron.

understanding of the mechanism through which impurities alter the morphology. Their experimental observations revealed that NaCl develops the unstable<sup>48</sup> face, which leads to octahedral crystals if organic additives are added. A schematic diagram for the change in the shape of an alkali halide crystal from cubic to octahedron and dodecahedron is shown in Fig. 3. The study have further concluded that the possibility of obtaining<sup>48</sup> surfaces of NaCl crystals grown from pure water solutions was an artifact of the earlier report. Their studies include the importance of the interaction of additives with the surfaces of NaCl, along with the volume and shape of the additive molecules towards the stabilization of unstable planes like  $\{111\}$  by the adsorption process. The adsorption of inorganic ions on the surfaces of NaCl crystals was also suggested to be important in controlling the morphology of rock salt.

The size and shape of NaCl crystals can have a profound bearing on basic properties such as their free-flow nature and dissolution features. Based on the chemical bonding theory of single-crystal growth, NaCl crystallizes in cubic form. Compared to spherical morphology, cubic morphology has certain disadvantages, the flow characteristics are inferior and the crystals are more liable to caking as a result of the larger contact area. Caking causes major problems when handling large quantities, and therefore, in parallel with the expedition for perfect cubic crystals, there has been constant exploration for modification of the morphology of NaCl. The cubic shape of NaCl occurs because of the slow growth of the  $\{100\}$  crystallographic faces.<sup>56,57</sup> In the last four to five decades, various methods have been reported for changing the morphology of NaCl crystals grown from solution.<sup>58</sup> Among them, the use of impurities is one of the most commonly adopted methods.<sup>59</sup> The reports suggest that the adsorption of impurities onto crystal faces alters the free energy of the surface and influences the growth of different sites in the crystal lattice. Such factors in turn disturb the growth kinetics and, subsequently, change the habit of the crystalline phase.<sup>6,60</sup> It is well known that solution-grown NaCl crystals usually show a richer morphology compared with those obtained from the vapor growth. Beside the cube, the  $\{111\}$  octahedron and dodecahedron  $\{110\}$  occur both in the presence of surface-specific impurities and under distinct supersaturations in pure aqueous solution. Prof. Thrailkill in



**Fig. 4** Photo-micrographs of NaCl crystals grown from: (A) 15 g glycine per 100 g water saturated with NaCl; (B) solution used in 'A' adjusted to pH 1.3 with hydrochloric acid; (C) solution used in 'A' adjusted to pH 10.8 with sodium hydroxide; (D) 40 g pyridinic betaine per 100 g of water saturated with NaCl; (E) solution used in 'D' with one equivalent of hydrochloric acid added. Reproduced with permission from ref. 61. Copyright 1949 American Chemical Society.

1949 first reported that dipolar ions modify the habit of NaCl crystals.<sup>61</sup> It was observed that in virtue of the dipolar character, the amino acids will interact with growing NaCl crystals and that would lead to crystal habit modification by almost any amino acid. The study was carried out with glycine, pyridine betaine, and  $\beta$ -alanine additives to modify the crystal habit of growing NaCl; the first causes the formation of dodecahedron crystals, while the latter two give octahedron crystals (Fig. 4).

In 1966 Phoenix and his research group published an extensive list of chemicals that are active in the aqueous NaCl solution and modify the normal cube-shaped NaCl crystals to needles, dendrites, and octahedra morphology. In the presence of a low concentration of  $[\text{Fe}(\text{CN})_6]^{4-}$  perfect cubic-shaped NaCl crystals are grown. However with the increase in  $[\text{Fe}(\text{CN})_6]^{4-}$  concentration star-shaped crystals are formed, with "dendritic" outgrowths from each of the eight corners of a central cube. The horny outgrowths of star-shaped crystals are made up of perfect cubes of diminished sizes at the end. Furthermore, at a very high concentration of  $[\text{Fe}(\text{CN})_6]^{4-}$  ( $2.8 \times 10^{-4}$  molal) the morphology of NaCl crystals changes abruptly into plate-like crystals.<sup>62</sup> Later in 1975 the same research group reported that the nitrilotriacetamide additive causes dendritic growth of NaCl crystals. The sizes of the cubic crystal blocks in the dendritic branches of NaCl are inversely proportional to the concentrations of nitrilotriacetamide. The results showed that nitrilotriacetamide causes the skeleton-type growth of NaCl, namely cubes or rectangular prisms presumably formed in the solution and piled up to make the structure.<sup>63</sup>

In 1981 Davey and his research group reported the effect of the crystallisation of NaCl in the presence of two biological polymers obtained from seaweeds. The polysaccharide additives carrageen moss extract (mixture of  $\lambda$  and  $\kappa$  carrageenans) and sodium alginate suppress the nucleation and increase the mean size of the NaCl crystal. These two biopolymers inhibit primary heterogeneous nucleation by adsorption onto, and deactivation of, active foreign surfaces. Additionally, it influences the secondary nucleation by adsorption onto the crystal surface, allowing dislocation growth to dominate over edge nucleation and producing NaCl crystals which are less susceptible to attraction. They adsorbed both on the crystal surfaces and on the motes

present in the solution. The crystal morphology practically suggests that the additives hinder edge nucleation and therefore allow dislocation growth to become the dominant growth mechanism.<sup>64</sup>

It is known that potassium ferrocyanide as an additive offers dendritic crystals and is used for the anticaking properties of NaCl (ref. 65 and 66). Prof. Bode has applied the surface X-ray diffraction technique to study the anticaking activity of ferrocyanide on NaCl explained by charge mismatch.<sup>67</sup> Their experiments showed that the ferrocyanide ion replaces a chloride ion on the  $\{100\}$  surface of NaCl and blocks further growth of the NaCl crystal due to the difference in ion charge. The presence of ferrocyanide in the crystal lattice prevents the growth of cubic crystals and leads to dendritic crystals inhibiting caking of salt crystals. Based on this charge mismatch interaction, it has been suggested as a blocking mechanism for the crystal growth of NaCl crystals by ferrocyanide.

A useful approach was developed to recycle the organic additive, glycine, as a habit modifier to harvest rhombic dodecahedron-shaped NaCl crystals from solar salt production from natural brines.<sup>68</sup> The  $[100]$  faces of NaCl grow faster than  $[110]$  faces in the presence of glycine, ultimately leading to the production of rhombic dodecahedron habit consisting of only  $[110]$  faces. Additionally, the inter-crystal contact area in the cubic form is significantly reduced in the regular rhombic dodecahedron form (Fig. 5).

Ghosh *et al.* have developed a simple method for the crystallization of nearly spherical polycrystalline NaCl particles in the size range of 300–1000  $\mu\text{m}$  at 55–60  $^\circ\text{C}$  by using an appropriate crystallizer fitted out with a butterfly wing-shaped impeller functioning at 250 rpm (Fig. 6).<sup>69</sup> The particle size as well as the conducive flow patterns depend on

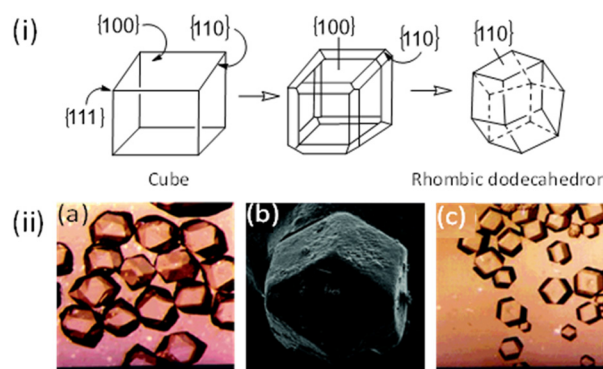


**Fig. 5** (i) Transformation of NaCl crystals from cube to rhombic dodecahedron via octadecahedron in the presence of glycine as a crystal habit modifier. (ii) (a) Rhombic dodecahedron crystals of NaCl grown using glycine (25% w/v), (b) SEM of an isolated rhombic dodecahedron NaCl crystal depicting regular rhombic  $[110]$  faces (six faces can be seen from this view), and (c) rhombic dodecahedron crystals of NaCl grown from subsoil brine using glycine (25%). Reproduced with permission from ref. 68. Copyright 2006 American Chemical Society.

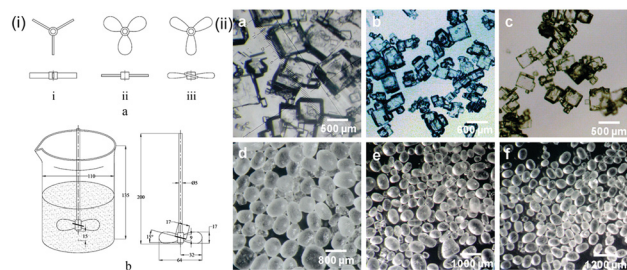


**Fig. 6** (i) Schematic drawings of (a) different types of impeller blades studied in the present work [( $\alpha$ ) pitch blade, ( $\beta$ ) flat propeller blade, and ( $\gamma$ ) butterfly wing-shaped blade] and (b) details of laboratory-scale experimental setup and dimensions of the butterfly wing-shaped blade identified for spherical salt preparation. The length scale is in mm and the angular scale in degrees. (ii) Optical microscopy images of cubic salt crystals obtained through crystallization of (a) synthetic, (b) sea, and (c) subsoil brines in an open beaker under gentle magnetic stirring at 55 °C. When the experiments were repeated using a special impeller operating at 250 rpm—while maintaining all other conditions identical—spherical salt particles shown in (d)–(f), respectively, were obtained. Reproduced with permission from ref. 69. Copyright 2010 American Chemical Society.

stirring speed, impeller design, and evaporation temperature. No habit modifiers were used for the “rounding” process. This sieved spherical salt exhibits superior flow (*ca.* 20% greater mass flow rate through a funnel; angle of repose around 16°) as compared to commercial vacuum evaporated free flow cubic salt of similar measurement. Additionally, the use of ethanol as an antisolvent during the process lowers the size distribution of the spherical salt particles. This process was scaled up to 10 kg levels for conventional edible and industrial applications.

A systematic study was undertaken to understand the role of impurities in controlling the morphology of NaCl crystals using computational and experimental studies. The report on the conformational behaviors of urea and glycineamide in the solvent medium with the important surfaces of NaCl is noteworthy.<sup>70</sup> The additives such as urea and glycineamide possess similar functional groups, however, the influence on the morphology of salt crystals is largely different. Cluster model calculations indicate that the amide group interacts with both  $\text{Na}^+$  and  $\text{Cl}^-$  ions on the {100} surface, while the carbonyl oxygen of these compounds interacts with sodium

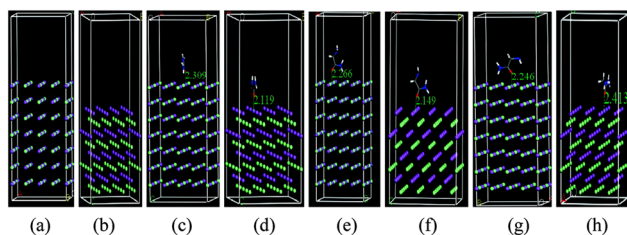


**Fig. 7** {100} and {111} NaCl surface slab model (a and b). LDA/PWC/DND calculated geometries of urea II (c and d) and glycineamide conformers IV (e and f) and VI (g and h) with the {100}/{111} surface of NaCl in slab models (purple, sodium; green, chlorine; red, oxygen; blue, nitrogen; and white, hydrogen). Reproduced with permission from ref. 70. Copyright 2007 American Chemical Society.

ions on the {111} surface. Urea tends to interact with the {111} surface of sodium chloride in both gas and aqueous phases, which aligns with observations that it can inhibit growth on this plane, leading to a transformation in NaCl crystal habit from cubes to octahedra. In contrast, glycineamide conformers favor the stable {100} surface of sodium chloride in water, showing little to no impact on the crystal morphology of sodium chloride (Fig. 7).

To investigate the molecular size fitting to the crystal lattice of NaCl, density functional theory (DFT) was performed with formamide on the lattice planes of alkali halides [ $d\{100_{\text{LiF}}\} = 2.02 \text{ \AA}$ ;  $d\{100_{\text{NaCl}}\} = 2.82 \text{ \AA}$ , and  $d\{100_{\text{KI}}\} = 3.51 \text{ \AA}$ ] and its impact on the morphology of such alkali halides (LiF, NaCl, and KI) crystals.<sup>71</sup> The theoretical calculations were performed both in gas and aqueous phases by using a continuum model (COSMO/COSMO-RS). The results suggest that the amide functional group of formamide ( $\text{CONH}_2$ ) interacts with {100} and {110} planes of NaCl whereas the carbonyl functionality interacts with the {111} surface (Fig. 8). The  $-\text{NH}$  functionality of formamide binds to the chloride ion, and the carbonyl functional group interacts with the sodium ion of the {100} and {110} planes. For NaCl, the lattice distance of (2.82 Å) fits with the distance of formamide (2.53 Å) and maximizes its interaction on top of the sodium ion with the {111} plane. However, for smaller lattice size LiF, the formamide binds with the {110} and {100} planes (lattice distance; LiF is 2.025 Å) by squeezing the N–H and C=O bond distance from 2.53 Å to  $\sim 2.45 \text{ \AA}$  and the {111} plane of LiF interacts with formamide in a similar fashion to that observed for NaCl (Fig. 8). However, in contrast to LiF, the formamide maximizes its interaction with

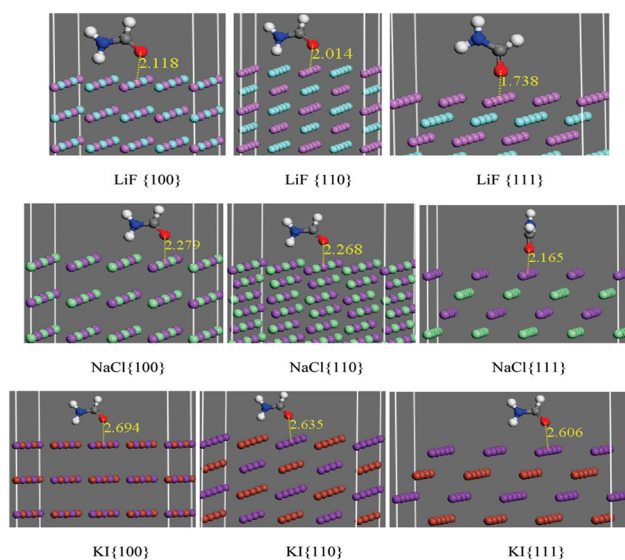


**Fig. 8** LDA/PWC/DND-calculated geometries of formamide with {100}, {110}, and {111} surfaces of NaCl, LiF, and KI in the slab model (purple: sodium, lithium, and potassium; green: chlorine and fluorine; brown: iodine; red: oxygen; blue: nitrogen; white: hydrogen). It is reproduced with permission from ref. 71. Copyright 2009 American Chemical Society.

the much larger {100} and {110} surfaces of KI (lattice distance; KI is 3.5 Å) by stretching the equilibrium distance between the carbonyl oxygen atom and the –N–H hydrogen from 2.53 Å to 2.57 Å. Therefore, formamide espouses its geometry to maximize the interaction with the specific surfaces of these alkali halides, and the molecular size fitting became less important in these cases. Furthermore, it has been observed that the solvation energy plays a major role in the interaction energies whereas the matching of the size of the additive with the neighboring ion spacing on the lattice planes of the different alkali halides is less important. The calculated values using slab models indicate that, in an aqueous solution, formamide interacts favorably with the {111} surface of NaCl ( $\Delta E$ )  $-23.8 \text{ kcal mol}^{-1}$  for {111} vs.  $-0.4$  and  $-4.3 \text{ kcal mol}^{-1}$  for {100} and {110}, respectively and helps the formation of octahedral-shaped crystals. Meanwhile, for LiF, the interaction of formamide with all the surfaces is found to be repulsive in the aqueous solution, and in the case of KI, the interactions are very weak ( $\sim -2$  to  $-5 \text{ kcal mol}^{-1}$ ) on all surfaces, *i.e.*, no distinct effect of formamide on crystal morphology is observed.

In 2009, the same research group reported the influence of citric acid under different pH conditions on habit modification of rock salt by employing DFT calculations.<sup>72</sup> The composition analysis at different pH values showed the importance of anionic forms of citric acid towards the morphological feature of sodium chloride. The slab model calculations indicate that the dihydrogen citrate is required to modify the morphology of sodium chloride from cubic to octahedron. After observing the function of citric acid, having three carboxylic groups (analogous to NTA) as a habit modifier for NaCl, the influence of NTA on the habit of NaCl salt crystals was examined computationally and

experimentally.<sup>73</sup> Earlier it was reported that NTA has no role in the growth habit of NaCl crystals.<sup>74</sup> Both the experimental and computational results suggest that the NTA prefers to interact more strongly with the stable {100} surface of NaCl compared to the {111} surface; however, a greater preference for the {111} surface was observed with the  $\text{NTA}^{-1}$ ,  $\text{NTA}^{-2}$ , and  $\text{NTA}^{-3}$  derivatives. The calculated interaction energies show that at least  $\text{NTA}^{-1}$  is necessary to influence the habit of NaCl from cubes to octahedra. The interaction energy differences are much larger in favor of the {111} plane of NaCl with  $\text{NTA}^{-2}$  and  $\text{NTA}^{-3}$ , supporting the observed experimental results at higher pH between 3.0 and 14.0. In general, the interactions of NTA and its dissociated forms with NaCl surfaces involve several carboxyl groups (Fig. 9). Interestingly, as predicted by the MESP analysis, it was also revealed that the nitrogen center of  $\text{NTA}^{-3}$  was engaged in the interaction with the {111} plane of NaCl.

The slab model calculations corroborate the composition analysis results in which the  $\text{NTA}^{-1}$ ,  $\text{NTA}^{-2}$ , and  $\text{NTA}^{-3}$  species play a pivotal role in altering the morphology of NaCl crystals from cubes to octahedra under various pH conditions (Fig. 9).

It has been reported that a single additive (barbituric acid) can give dual morphology of rock-salt crystals. Barbituric acid was very effective in a trace amount (0.08–0.2% w/v) in inducing rhombic dodecahedron NaCl crystals, and can be useful for real practical applications.<sup>75</sup> The computational studies suggest that at lower pH values ( $\text{pH} \approx 3$ ) barbituric acid will form rhombic dodecahedron crystals whereas at higher pH values ( $\text{pH} \approx 8$ ) octahedron crystals will be formed, which has been further confirmed by the experimental studies. Barbituric acid preferentially interacts with the {110} planes of NaCl compared to {100} and {111} planes (Fig. 10). The –CONH and –COCH<sub>2</sub> functional groups of barbituric acid bind stronger to the {100} and {110} planes

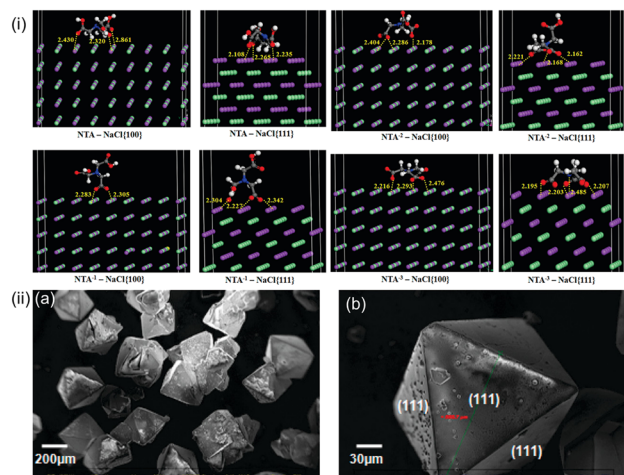


**Fig. 9** (i) LDA/PWC/DND-calculated geometries of NTA,  $\text{NTA}^{-1}$ ,  $\text{NTA}^{-2}$ , and  $\text{NTA}^{-3}$  with {100} and {111} surfaces of NaCl, in the slab model (purple: sodium, green: chlorine gray: carbon; red: oxygen; blue: nitrogen; white: hydrogen). (ii) SEM images of bulk (a) and single (b) octahedron crystals of NaCl grown at  $\text{pH} = 2.7$  in the presence of NTA as an additive. Reproduced with permission from ref. 73. Copyright 2011 American Chemical Society.

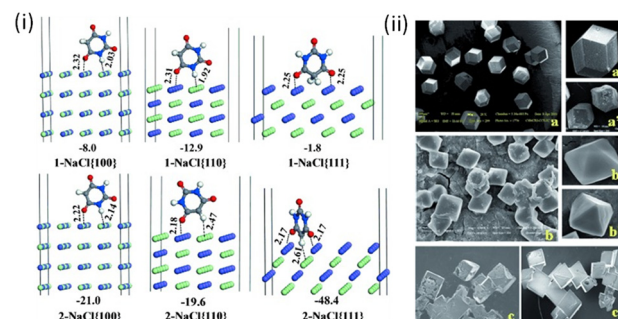


**Fig. 10** (i) GGA/PW91/DNP//LDA/PWC/DND calculated geometries and interaction energies (in COSMO) of 1 and 2 with the {100}, {110}, and {111} surfaces of NaCl are given in  $\text{kcal mol}^{-1}$ . Distances are given in Å (purple sodium, green chloride, gray carbon, red oxygen, blue nitrogen, white hydrogen). (ii) The SEM images for the NaCl crystals in the presence of barbituric acid at different pH values, a)  $\text{pH} 3.0$ , a')  $\text{pH} 3.2$ , b)  $\text{pH} 6.0$ , b')  $\text{pH} 10$ , c)  $\text{pH} 12.0$ , and c') without the additive at  $\text{pH} 7.0$  (the additive can also be called an impurity as it is added in a pure solution of NaCl). It is reproduced with permission from ref. 69. Copyright 2012 John Wiley and Sons.

of NaCl. The interaction of barbituric acid with  $\{111\}$  is much weaker than that of corresponding  $\{100\}$  and  $\{110\}$  planes (Fig. 10). These theoretically calculated results suggest that barbituric acid encourages the habit modification of NaCl to rhombic dodecahedron crystals. Meanwhile for its ionic form, the  $(-\text{COCH}^-)$  functionality more effectively interacts with the  $\{110\}$  plane, and the  $-\text{CONH}$  group binds with the  $\{100\}$  plane (Fig. 10). The calculated results indicate the stronger binding of its ionic form with  $\{111\}$  which leads to the formation of octahedron crystals. This combined approach of computational predictions followed by experimental validation appeared to be a practical manner for designing new additives.

Townsend *et al.* have studied the influence of various polymeric additives (poly(vinyl alcohol), polyacrylamide, and lysozyme) on the habit modification and anti-caking of NaCl crystals grown from saturated aqueous solution.<sup>76</sup> The experimental results showed that polymer additives comprising an amide functional group induce  $\{111\}$  face formation on NaCl crystals with a one to two orders of magnitude stronger effect than that of the analogous monomer. Polyacrylamide partly blocks the growth of the NaCl crystal on the  $\{111\}$  face, consequently allowing the  $\{100\}$  faces to grow comparatively faster, leading to a crystal with  $\{111\}$  facets with trigonal-shaped island morphology (Fig. 11). Meanwhile, the alcohol functional group does not affect the habit or surface modification and the NaCl crystals remain cubic. Furthermore, all these polymers led to macrostep formation and work as nucleation inhibitors, which leads to the formation of low-density larger-sized crystals. Among poly(vinyl alcohol) and polyacrylamide, poly(vinyl alcohol) showed enhanced caking, whereas polyacrylamide doesn't show any significant anticaking effect.

Prof. Vlieg and his research group reported ultrathin crystal needle morphology during the evaporation of saturated aqueous NaCl solution in the presence of amide-containing additives (nitrilotriacetamide, methylglycine diacetamide, and glutamic acid diacetamide) (Fig. 12).<sup>77</sup> The formation of thin, elongated NaCl needle crystals is unexpected for the cubic  $43m$  point group symmetry of NaCl.

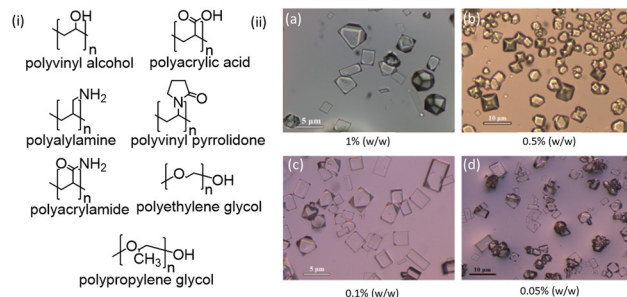


**Fig. 11** (i) Polymers used in this investigation as potential modifiers of NaCl morphology and caking. (ii) Small-scale *in situ* experiments with polyacrylic acid additive (a–d). Reproduced with permission from ref. 76. Copyright 2015 American Chemical Society.

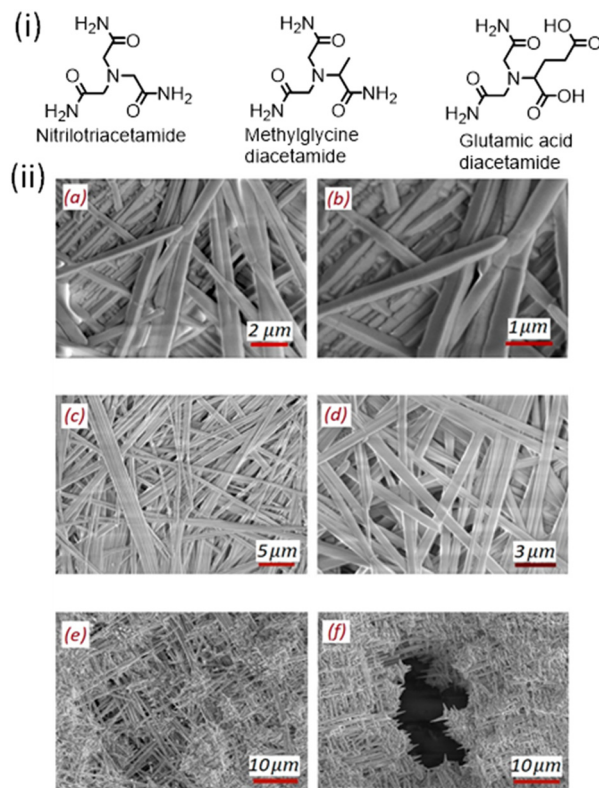


**Fig. 12** (i) Structures of the amide compounds used in this investigation. (ii) Detailed SEM views of needle-shaped crystals obtained from a saturated brine solution containing (a and b) 1% (w/w) nitrilotriacetamide, (c and d) 1% (w/w) methylglycine diacetamide, and (e and f) 1% (w/w) glutamic acid diacetamide. Reproduced with permission from ref. 77. Copyright 2018 American Chemical Society.

They have observed that the evaporation of saturated brine solution with additives of  $\sim 1\%$  (w/w) methylglycine diacetamide, nitrilotriacetamide, and glutamic acid

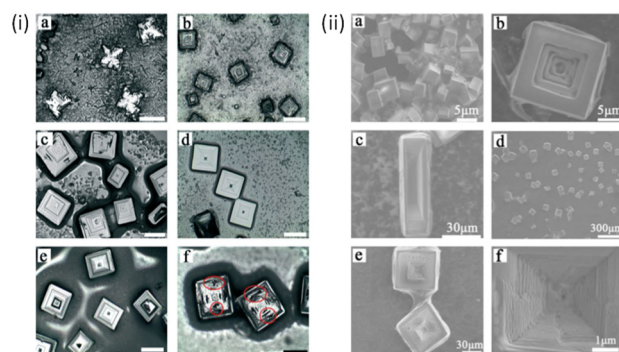


**Fig. 13** (i) Optical micrographs of NaCl crystals prepared at NaCl concentrations of (a) 0.1 mol L<sup>-1</sup>, (b) 0.25 mol L<sup>-1</sup>, (c) 0.50 mol L<sup>-1</sup>, (d) 1.00 mol L<sup>-1</sup>, (e) 1.50 mol L<sup>-1</sup> and (f) 2.0 mol L<sup>-1</sup>. Scale bar = 160 μm. (ii) SEM images of NaCl crystals (a) without DNA, (b and c) with 100 μmol L<sup>-1</sup> DNA-1 and 1.5 mmol L<sup>-1</sup> silver nitrate, and (d–f) with 100 μmol L<sup>-1</sup> DNA-2 and 1.5 mmol L<sup>-1</sup> silver nitrate. The DNA sequences of DNA-1 is: 5'-CCCCCCCCCCCC(T...T)43-3' and that of DNA-2 is: 5'-CCCC CC(T...T)50-3'. Reproduced with permission from ref. 78. Copyright 2017 Royal Society of Chemistry.

diacetamide produced a dense layer of ultrathin crystal needles, 0.3–2  $\mu\text{m}$  wide. These “criss-cross” pattern needles are formed from cubic NaCl, with no evidence of enormous amounts of amide in the composition. In the presence of these amide containing additives, the {100} top face of NaCl grows fast, whereas the symmetry equivalent (010)/ (0 $\bar{1}$ 0) and (001)/ (00 $\bar{1}$ ) side faces of the cubic crystal do not grow at all. Therefore, the tip formation is induced by morphological instability followed by time-dependent adsorption of these additives blocking the growth of the needle side faces.

It has been reported that DNA can act as a habit modifier to prepare uniform hopper-like NaCl crystals *via* the solvent evaporation method.<sup>78</sup> Fig. 13 shows that single-stranded DNA and double-stranded DNA can induce the change in the NaCl crystals to grow into hopper-like and dendritic-like crystals, respectively. Since the {111} face of the NaCl crystal is relatively polar compared to {100} hence the interactions of DNA are stronger with the former face inducing the octahedron crystal of NaCl. Moreover, the addition of silver ions affects the distribution of DNA, hence affecting the adsorption of DNA on NaCl {100}, resulting in reduced size of the hopper-like crystals (Fig. 13).

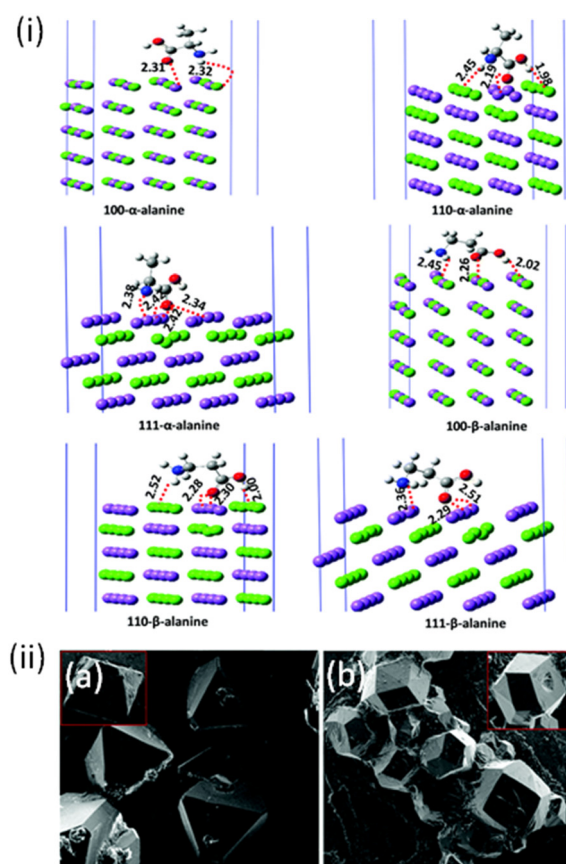


**Fig. 14** (i) LDA/PWC/DND calculated geometries of  $\alpha$ - and  $\beta$ -alanine with the {100}, {110}, and {111} surfaces of NaCl (distances are given in Å) (purple: sodium, green: chloride, gray: carbon, red: oxygen, blue: nitrogen, white: hydrogen). (ii) SEM images for the NaCl crystals in the presence of  $\alpha$ -alanine (a) and  $\beta$ -alanine (b). Reproduced with permission from ref. 79. Copyright 2018 Royal Society of Chemistry.

Recently, it has been reported that additives such as (alanine) can give two different morphologies of rock-salt crystals in the presence of its two isomers ( $\alpha$  and  $\beta$  alanine).<sup>79</sup> The computational studies indicate that both the isomers of alanine can act as habit modifiers, whereby  $\alpha$ -alanine changes the morphology of salt crystals to an octahedron, and  $\beta$ -alanine should give a rhombic dodecahedron. The computational predictions were validated by experimental studies (Fig. 14). According to the computational results,  $\alpha$ -alanine interacts with the {111} plane of the NaCl crystal through the electron rich site of the nitrogen of the amine functional group and the two oxygen sites of the carboxylic acid functionality. The molecular electrostatic potential surface calculation of  $\alpha$ -alanine indicates that there is a negative potential on the nitrogen and two carboxylic oxygen atoms and a positive electrostatic potential on the two amine hydrogens. The  $\alpha$ -alanine takes advantage of these three negative sites to interact with the {111} plane of NaCl. However, the {110} and {100} planes contain  $\text{Na}^+$  and  $\text{Cl}^-$  on the top of the NaCl surface, which bind to amine hydrogen and carbonyl oxygen atoms respectively. Meanwhile for  $\beta$ -alanine, the {110} plane interacts more strongly than {100} and {111} faces and hence forms rhombic dodecahedron crystals (Fig. 14). Applications for these morphological salt crystals with alanine isomers range from the food to pharmaceutical industries. The free-flowing ability of the NaCl salt crystals with cubic, octahedron, and rhombic dodecahedron morphologies has been demonstrated in the video clipping given in the reported article.<sup>79</sup>

Later 2-amino-pentanoic acid and 1-pyridiniumylacetate were also examined as crystal habit modifiers for NaCl. The computational results show that the carboxylic acid and amine functionality of 2-amino-pentanoic acid strongly interact with the {110} plane of NaCl compared with {100} and {111} planes (Fig. 15).<sup>80</sup> Therefore, the preferential interaction of 2-amino-pentanoic acid with the {110} plane of NaCl forms rhombic dodecahedron NaCl crystals. However, the interaction of 1-pyridiniumylacetate with the surfaces of NaCl is different compared to 2-amino-pentanoic acid. The anionic carboxyl functionality of 1-pyridiniumylacetate strongly interacts with the {111} plane of NaCl compared to {100} and {110} planes. The interactive distances are given in Fig. 15. Consequently, 1-pyridiniumylacetate interacts with the {111} plane preferentially compared to {100} and {110} plane and yields octahedron morphology of NaCl crystals (Fig. 15).

Very recently, Prof. Fontana *et al.* discussed the growth of NaCl under microgravity and compared them with earth-grown NaCl hopper cubes including naturally occurring hopper cubes grown through geologic processes in brine-soaked mud (Fig. 16).<sup>81</sup>

Hopper cube morphology forms when the mass transport to the center of the crystal happens slower and the edges continue to grow faster. In nature, hopper growth of cube faces is improved when the face growth is arrested by

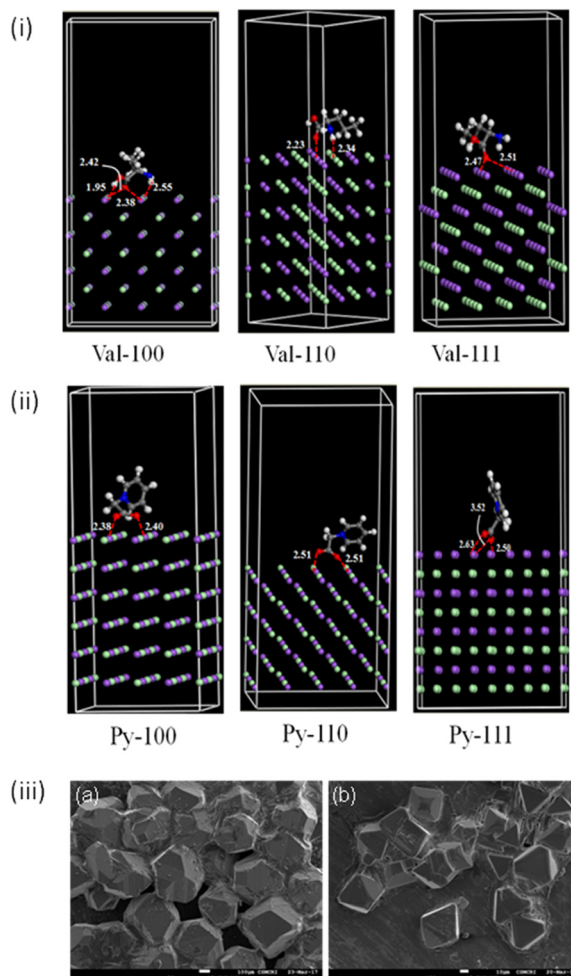


**Fig. 15** The optimized geometry of (i) 1-pyridiniumylacetate and (ii) 2-amino-pentanoic acid with the planes of NaCl ( $\{100\}$ ,  $\{110\}$ , and  $\{111\}$ ) at LDA/PWC/DND method (distances are given in Å) (purple: sodium, green: chloride, grey: carbon, red: oxygen, blue: nitrogen, white: hydrogen) [Py = 1-pyridiniumylacetate, and Val = 2-amino-pentanoic acid]. (iii) The SEM images for the NaCl crystals in the presence of 2-amino-pentanoic acid (a) and 1-pyridiniumylacetate (b). Reproduced with permission from ref. 80. Copyright 2019 Elsevier.

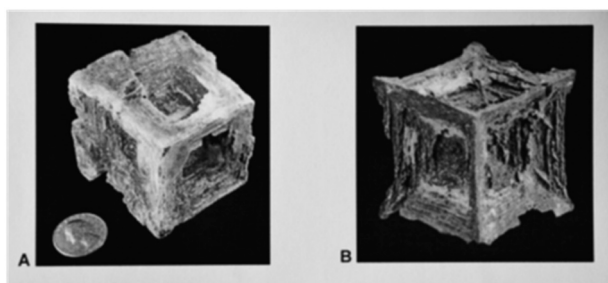


**Fig. 16** (A) Displacively in mud-grown halite hopper and a pseudomorph after halite displacively grown halite hopper ( $6.3 \times 6.3 \times 6.3$  cm) with mud inclusions. (B) Hopper shaped calcite pseudomorph after halite was covered with reddish-brown limonite ( $3 \times 3 \times 3$  cm). Reproduced with permission from ref. 81. Copyright 2019 Nature.

microgravity and terrestrial gravity hopper growth conditions are low supersaturation and slower growth rates over long periods. Here naturally occurring symmetrical NaCl hopper cubes of larger size (1–20 cm) are suspended in brine-soaked mud, assumed to be produced in a slow-growth, diffusion-dominated environment.

## 2. Summary and outlook

Controlling crystal morphology is an important area of research in academia and industry because of its significant impact on the physical properties of crystalline materials. It has been observed that the external appearance of the crystal, that is, its habit, is affected by the rate of crystallization and by the presence of impurities. In the 1950s crystal habit modifiers of very diverse character, *e.g.*, multivalent cations, complexes, soluble polymers, surface active agents, fine particles of sparingly soluble salts, and biologically active macromolecules, were used to change the morphology of NaCl crystals. The selection of additives to influence the NaCl crystals has been empirical and several organic molecules (amino acids, peptides, DNA, polymers, *etc.*) and inorganic complexes have been used as impurities to modify the habit of NaCl crystals.

In recent years, the studies performed to understand the habit modification of NaCl crystals at the molecular level employed theoretical/computational and experimental methods. The role of additives in affecting the habit of NaCl crystals was recognized with lattice fit, multipoint adsorption, and conformations of the additives. Theoretical models were also developed *i.e.*, the Bravais–Friedel–Donnay–Harker model, attachment energy model, modified attachment energy model, occupancy model, spiral growth model, 2D nucleation model, step-pinning model, and spiral-pinning model to rationalize and understand conditions that can yield a desired crystal habit of crystals including the NaCl crystals. The quantum chemical and molecular dynamics simulations have contributed to understanding the microscopic details of crystal formations and to predicting the morphology with newly designed additives. The recent efforts combining the experimental and computational techniques qualitatively elucidated the role of habit modifiers in inducing the morphology of sodium chloride salt crystals. This is the beginning of a complex research problem, where many additional external parameters are needed to be incorporated in the theoretical models to understand and predict the morphologies of sodium chloride crystals in a quantitative manner. The systematic experimental work not only with organic additives, but with inorganic additives as well for large scale data set in conjunction with machine learning would be of benefit to the development of the crystallization process for sodium chloride in particular and for other ionic systems in general. The applications of the modified NaCl crystals can have much larger impact on the growth of the salt industries and other practical applications such as tissue engineering.

interactions with mud particles or with adsorbed impurities from the solution. The major differences between

## Author contributions

S. K. P. – conceptualization, investigation, writing – original draft, writing – review & editing; B. G. – conceptualization, investigation, writing – original draft, writing – review & editing.

## Conflicts of interest

There are no conflicts to declare.

## Acknowledgements

We acknowledge DST, New Delhi and CSIR-CSMCRI, Bhavnagar to support this work. We also acknowledge the work carried out by the PhD students involved in this project. We thank the reviewer's for their insightful suggestions and comments that improved the manuscript. PRIS no 13/2025 has been assigned for this manuscript.

## Notes and references

- 1 S. L. Baldochi and I. M. Ranieri, in *Encyclopedia of Materials: Science and Technology*, ed. K. H. J. Buschow, R. W. Cahn, M. C. Flemings, B. Ilschner, E. J. Kramer, S. Mahajan and P. Veyssière, Elsevier, Oxford, 2001, pp. 74–78, DOI: [10.1016/B0-08-043152-6/00014-0](https://doi.org/10.1016/B0-08-043152-6/00014-0).
- 2 S. J. Urwin, G. Levilain, I. Marziano, J. M. Merritt, I. Houson and J. H. Ter Horst, *Org. Process Res. Dev.*, 2020, **24**, 1443–1456.
- 3 M. A. McDonald, H. Salami, P. R. Harris, C. E. Lagerman, X. Yang, A. S. Bommaris, M. A. Grover and R. W. Rousseau, *React. Chem. Eng.*, 2021, **6**, 364–400.
- 4 P. Klitou, I. Rosbottom, V. Karde, J. Y. Y. Heng and E. Simone, *Cryst. Growth Des.*, 2022, **22**, 6103–6113.
- 5 R. Speidel, *Neues Jahrbuch fur Mineralogie*, 1961, vol. 4, pp. 81–93.
- 6 J. McGinty, N. Yazdanpanah, C. Price, J. H. ter Horst and J. Sefcik, in *The Handbook of Continuous Crystallization*, The Royal Society of Chemistry, 2020, pp. 1–50, DOI: [10.1039/9781788013581-00001](https://doi.org/10.1039/9781788013581-00001).
- 7 I. Rosbottom, C. Y. Ma, T. D. Turner, R. A. O'Connell, J. Loughrey, G. Sadiq, R. J. Davey and K. J. Roberts, *Cryst. Growth Des.*, 2017, **17**, 4151–4161.
- 8 R. T. Prider, in *Mineralogy*, Springer US, Boston, MA, 1983, pp. 106–114, DOI: [10.1007/0-387-30720-6\\_31](https://doi.org/10.1007/0-387-30720-6_31).
- 9 J. D. Dunitz and J. Bernstein, *Acc. Chem. Res.*, 1995, **28**, 193–200.
- 10 F. Grepioni, *New J. Chem.*, 2008, **32**, 1657–1658.
- 11 K. Higashi, K. Ueda and K. Moribe, *Adv. Drug Delivery Rev.*, 2017, **117**, 71–85.
- 12 G. Clydesdale and K. J. Roberts, *AIChE Symp. Ser.*, 1991, **87**, 138–142.
- 13 Z. Berkovitch-Yellin, *J. Am. Chem. Soc.*, 1985, **107**, 8239–8253.
- 14 M. Bayer-Giraldi, G. Sazaki, K. Nagashima, S. Kipfstuhl, D. A. Vorontsov and Y. Furukawa, *Proc. Natl. Acad. Sci. U. S. A.*, 2018, **115**, 7479–7484.
- 15 P. Neugebauer, J. Cardona, M. O. Besenhard, A. Peter, H. Gruber-Woelfler, C. Tachtatzis, A. Cleary, I. Andonovic, J. Sefcik and J. G. Khinast, *Cryst. Growth Des.*, 2018, **18**, 4403–4415.
- 16 G. Neuroth and H. Klapper, *Cryst. Res. Technol.*, 2020, **55**, 1900159.
- 17 J. Orehek, D. Teslić and B. Likozar, *Org. Process Res. Dev.*, 2021, **25**, 16–42.
- 18 M. Yokota, E. Oikawa, J. Yamanaka, A. Sato and N. Kubota, *Chem. Eng. Sci.*, 2000, **55**, 4379–4382.
- 19 D. C. Green, R. Darkins, B. Marzec, M. A. Holden, I. J. Ford, S. W. Botchway, B. Kahr, D. M. Duffy and F. C. Meldrum, *Cryst. Growth Des.*, 2021, **21**, 3746–3755.
- 20 J. Fu, M. Zhang, K. Gao and H. Ren, *FirePhysChem*, 2023, **3**, 263–274.
- 21 H. Chen, S. Duan, Y. Sun, X. Song and J. Yu, *RSC Adv.*, 2020, **10**, 5604–5609.
- 22 I. Okada, Y. Namiki, H. Uchida, M. Aizawa and K. Itatani, *J. Mol. Liq.*, 2005, **118**, 131–139.
- 23 R. S. Ploss, *Science*, 1964, **144**, 169–170.
- 24 A. P. Ribeiro, M. H. Masuchi, E. K. Miyasaki, M. A. Domingues, V. L. Stroppa, G. M. de Oliveira and T. G. Kieckbusch, *J. Food Sci. Technol.*, 2015, **52**, 3925–3946.
- 25 J. Anwar and P. K. Boateng, *J. Am. Chem. Soc.*, 1998, **120**, 9600–9604.
- 26 D. Aquilano, R. Benages-Vilau, M. Bruno, M. Rubbo and F. R. Massaro, *CrystEngComm*, 2013, **15**, 4465–4472.
- 27 J. Prywer, *J. Cryst. Growth*, 2004, **270**, 699–710.
- 28 P. Hartman and W. G. Perdok, *Acta Crystallogr.*, 1955, **8**, 521–524.
- 29 P. Hartman and W. G. Perdok, *Acta Crystallogr.*, 1955, **8**, 49–52.
- 30 P. Hartman and P. Bennema, *J. Cryst. Growth*, 1980, **49**, 145–156.
- 31 J. W. Mullin, in *Crystallization*, ed. J. W. Mullin, Butterworth-Heinemann, Oxford, 4th edn, 2001, pp. 216–288, DOI: [10.1016/B978-075064833-2/50008-5](https://doi.org/10.1016/B978-075064833-2/50008-5).
- 32 R. Docherty and K. J. Roberts, *J. Cryst. Growth*, 1988, **88**, 159–168.
- 33 A. S. Myerson, in *Molecular Modeling Applications in Crystallization*, ed. A. S. Myerson, Cambridge University Press, Cambridge, 1999, pp. 55–105, DOI: [10.1017/CBO9780511529610.003](https://doi.org/10.1017/CBO9780511529610.003); R. Docherty and P. Meenan, in *Molecular Modeling Applications in Crystallization*, ed. A. S. Myerson, Cambridge University Press, Cambridge, 1999, pp. 106–165, DOI: [10.1017/CBO9780511529610.004](https://doi.org/10.1017/CBO9780511529610.004).
- 34 K. Sato, L. Bayés-García, T. Calvet, M. À. Cuevas-Diarte and S. Ueno, *Eur. J. Lipid Sci. Technol.*, 2013, **115**, 1224–1238.
- 35 X. Y. Liu, E. S. Boek, W. J. Briels and P. Bennema, *Nature*, 1995, **374**, 342–345.
- 36 C. W. Bunn and C. N. Hinshelwood, *Proc. R. Soc. London, Ser. A*, 1933, **141**, 567–593.
- 37 C. W. Bunn, *Proc. R. Soc. London, Ser. A*, 1933, **141**, 567–593.
- 38 C. W. Bunn and C. N. Hinshelwood, *Proc. R. Soc. London, Ser. A*, 1997, **141**, 567–593.
- 39 Z. Cai, Y. Liu, Y. Song, G. Guan and Y. Jiang, *J. Cryst. Growth*, 2017, **461**, 1–9.

- 40 Y. Zhu, M. Lu, F. Gao, C. Zhou, C. Jia and J. Wang, *Ind. Eng. Chem. Res.*, 2023, **62**, 4800–4816.
- 41 N. Cabrera and D. A. Vermilyea, The Growth of Crystals from Solution, in *Growth and Perfection of Crystals*, ed. R. H. Doremus, B. W. Roberts and D. Turnbull, Wiley, New York, 1958, pp. 393–410.
- 42 G. Bliznakov, *Bull. Acad. Bulg. Sci., Ser. Phys.*, 1954, **4**, 135–152.
- 43 G. W. Sears, *J. Chem. Phys.*, 2004, **29**, 1045–1048.
- 44 N. Albon and W. J. Dunning, *Acta Crystallogr.*, 1962, **15**, 474–476.
- 45 M. A. Larson and J. W. Mullin, *J. Cryst. Growth*, 1973, **20**, 183–191.
- 46 R. Davey, *Crystal Growth in Science and Technology*, 1989, pp. 217–224.
- 47 A. Sen, S. Barik, A. Singh and B. Ganguly, *Can. J. Chem.*, 2015, **93**, 1219–1225.
- 48 N. Radenović, W. V. Enckevert, P. Verwer and E. Vlieg, *Surf. Sci.*, 2003, **523**, 307–315.
- 49 R. Boistelle and B. Simon, *J. Cryst. Growth*, 1974, **26**, 140–146.
- 50 M. A. Boles, M. Engel and D. V. Talapin, *Chem. Rev.*, 2016, **116**, 11220–11289.
- 51 L. Royer, *C. R. Acad. Sci.*, 1934, **198**, 1868–1870.
- 52 J. H. Palm and C. H. MacGillavry, *Acta Crystallogr.*, 1963, **16**, 963–968.
- 53 M. Hille and C. Jentsch, *Z. Kristallogr.*, 1963, **118**, 283–290.
- 54 L. Lian, K. Tsukamoto and I. Sunagawa, *J. Cryst. Growth*, 1990, **99**, 150–155.
- 55 P. W. Tasker, *Philos. Mag. A*, 1979, **39**, 119–136.
- 56 J. Xu and D. Xue, *Acta Mater.*, 2007, **55**, 2397–2406.
- 57 X. U. Zhao, X. Ren, C. Sun, X. U. Zhang, Y. Si, C. Yan, J. Xu and D. Xue, *Funct. Mater. Lett.*, 2008, **1**, 167–172.
- 58 D. Xue, L. Zou, L. E. I. Wang and X. Yan, *Mod. Phys. Lett. B*, 2009, **23**, 3761–3768.
- 59 S. Al-Jibbouri and J. Ulrich, *Cryst. Res. Technol.*, 2001, **36**, 1365–1375.
- 60 F. Civati, C. O'Malley, A. Erxleben and P. McArdle, *Cryst. Growth Des.*, 2021, **21**, 3449–3460.
- 61 C. P. Fenimore and A. Thraillkill, *J. Am. Chem. Soc.*, 1949, **71**, 2714–2717.
- 62 A. Glasner and M. Zidon, *J. Cryst. Growth*, 1974, **21**, 294–304.
- 63 S. Sarig and F. Tartakovsky, *J. Cryst. Growth*, 1975, **28**, 300–305.
- 64 J. D. Birchall and R. J. Davey, *J. Cryst. Growth*, 1981, **54**, 323–329.
- 65 A. A. C. Bode, M. Verschuren, M. Jansen, S. Jiang, J. A. M. Meijer, W. J. P. van Enckevert and E. Vlieg, *Powder Technol.*, 2015, **277**, 262–267.
- 66 A. A. C. Bode, S. Jiang, J. A. M. Meijer, W. J. P. van Enckevert and E. Vlieg, *Cryst. Growth Des.*, 2012, **12**, 5889–5896.
- 67 A. A. C. Bode, V. Vonk, F. J. van den Bruele, D. J. Kok, A. M. Kerkenaar, M. F. Mantilla, S. Jiang, J. A. M. Meijer, W. J. P. van Enckevert and E. Vlieg, *Cryst. Growth Des.*, 2012, **12**, 1919–1924.
- 68 A. Ballabh, D. R. Trivedi, P. Dastidar, P. K. Ghosh, A. Pramanik and V. G. Kumar, *Cryst. Growth Des.*, 2006, **6**, 1591–1594.
- 69 I. Mukhopadhyay, V. P. Mohandas, G. R. Desale, A. Chaudhary and P. K. Ghosh, *Ind. Eng. Chem. Res.*, 2010, **49**, 12197–12203.
- 70 A. Singh, S. Chakraborty and B. Ganguly, *Langmuir*, 2007, **23**, 5406–5411.
- 71 A. Singh, M. K. Kesharwani and B. Ganguly, *Cryst. Growth Des.*, 2009, **9**, 77–81.
- 72 M. A. Shafeeuulla Khan, A. Sen and B. Ganguly, *CrystEngComm*, 2009, **11**, 2660–2667.
- 73 M. A. S. Khan, A. Singh, S. Haldar and B. Ganguly, *Cryst. Growth Des.*, 2011, **11**, 1675–1682.
- 74 S. Sarig, A. Glasner and J. A. Epstein, *J. Cryst. Growth*, 1975, **28**, 295–299.
- 75 A. Sen and B. Ganguly, *Angew. Chem., Int. Ed.*, 2012, **51**, 11279–11283.
- 76 E. R. Townsend, W. J. P. van Enckevert, J. A. M. Meijer and E. Vlieg, *Cryst. Growth Des.*, 2015, **15**, 5375–5381.
- 77 E. R. Townsend, W. J. P. van Enckevert, P. Tinnemans, M. A. R. Blijlevens, J. A. M. Meijer and E. Vlieg, *Cryst. Growth Des.*, 2018, **18**, 755–762.
- 78 Y. Qin, D. Yu and J. Zhou, *CrystEngComm*, 2017, **19**, 5356–5360.
- 79 M. K. Si, S. K. Pramanik, V. Hingu and B. Ganguly, *Phys. Chem. Chem. Phys.*, 2018, **20**, 17125–17131.
- 80 M. K. Si, S. K. Pramanik, V. Hingu and B. Ganguly, *J. Mol. Struct.*, 2019, **1175**, 728–733.
- 81 D. Pettit and P. Fontana, *npj Microgravity*, 2019, **5**, 25.